Available online at www.sciencedirect.com
SCIENCE DIRECT
Journal of Catalysis 230 (2005) 420–435
JOURNAL OF CATALYSIS
www.elsevier.com/locate/jcat

Highly efficient Pd–Sb–TiO_2 catalysts for the vapour phase acetoxylation of toluene to benzyl acetate

A. Benhmid, K.V. Narayana, A. Martin *, B. Lücke, S. Bischoff, M.-M. Pohl, J. Radnik, M. Schneider

Institut für Angewandte Chemie Berlin-Adlershof e.V. [1], *Richard-Willstätter-Str. 12, D-12489 Berlin, Germany*

Received 13 October 2004; revised 16 December 2004; accepted 17 December 2004

Available online 25 January 2005

Abstract

A series of Pd–Sb–TiO_2 (anatase) catalysts has been prepared over a wide range of Pd loadings from 0.5 to 20 wt% and tested for the selective vapour-phase acetoxylation of toluene to benzyl acetate at a reaction temperature of 210 °C and a pressure of 2 bar. The catalysts were characterised by nitrogen adsorption, XRD, XPS, and TEM. The BET surface areas and pore volumes were observed to decrease considerably with increasing Pd content of the catalysts. XPS revealed that there is loss of both Pd and Sb in the surface region in the used catalysts. The particle size of Pd (measured by TEM) is found to increase dramatically in the used catalysts compared with the fresh ones. Pd particle size is observed to exhibit a strong influence on the catalytic performance of the catalysts. The activity of the catalysts was found to increase continuously with increasing Pd loading, which is associated with an increase in the Pd particle size of the catalysts. The catalyst with 20 wt% Pd has been found to display the best performance, giving conversion of toluene as high as ca. 92 mol% with a benzyl acetate selectivity of 85%. Nevertheless, the solids were observed to deactivate with time on stream due to a considerable amount of coke deposition on the surface. However, the catalysts can be regenerated in air and reused for more number of cycles with consistent performance.

Keywords: Pd–Sb–TiO_2 catalysts; Acetoxylation; Toluene; TEM; XRD; XPS

1. Introduction

The direct partial oxidation of hydrocarbons via the gas-phase process is one of the most interesting and demanding fields in heterogeneous catalysis, mainly because of the environmental acceptability and sustainability of such processing. At the same time, it is also a big challenge because partial oxidised products have to be prevented from overoxidation, which easily runs to total oxidation products. The direct partial oxidation of methyl aromatics to their respective benzylic alcohols/aldehydes belongs to this field. Nevertheless, this reaction is often unselective, as the desired products undergo further consecutive or parallel reactions to by-products and total oxidation (CO_x) as mentioned above. This problem can be overcome to a considerable extent, however, if the partial oxidation is carried out in the presence of suitable catalysts and appropriate auxiliary reagents to produce stable end products. One such good example for producing stable end products appears to be acetoxylation of methyl aromatics, leading to esters that can be easily and quantitatively hydrolysed to produce valuable alcohols (Scheme 1). A number of these products are extensively used as flavouring agents, fragrances, and building blocks in pharmaceutical industries [1,2].

Acetoxylation of various aromatic compounds with methyl substituents, like toluene and *o*-, *m*-, and *p*-xylenes, is known from the literature (e.g., [1,2]). Methyl-substituted compounds with additional substituents like a hydroxyl group, an alkoxy group, a carboxylic group, and even an

* Corresponding author. Fax: +49 30 63 92 44 54.
E-mail address: a.martin@aca-berlin.de (A. Martin).
[1] A member of the EU-Funded Coordination Action of Nanostructured Catalytic Oxide Research and Development in Europe (CONCORDE).

0021-9517/$ – see front matter
doi:10.1016/j.jcat.2004.12.019

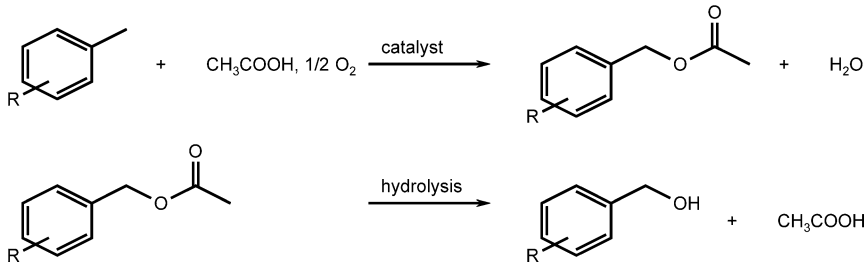

Scheme 1.

alkyl group with different side chain lengths can also be used as starting materials for acetoxylation reactions [3] to produce corresponding esters in a single step. The simplest compound in this family is benzyl acetate, which is a natural substance found in plants such as jasmine, hyacinth, gardenias, azaleas, and so on. It is used chiefly in the perfume industry, the food industry, and the chemical industry, notably as a solvent for cellulose acetate. The global demand for benzyl acetate ranges between 5000 and 10,000 tons per annum.

Literature reports [4,5] indicate that Pd-based catalysts are commonly used for the acetoxylation of (i) methyl aromatics [6–8], (ii) halo aromatics [9], and (iii) naphthalene [10]. It is known from the literature that Pd-based catalysts are also active for the acetoxylation of aliphatics like ethylene [11] and propylene [12].

The majority of the research reported so far was carried out mostly under liquid-phase conditions and in batch reactors [4,9]. A study by Miyake et al. [13], intended to improve the catalyst life over Pd–Bi–SiO_2 catalysts, resulted in only 10% conversion of toluene. Benazzi et al. [6] and Ebitani et al. [14] claimed yields of benzyl acetate as high as 77% (100% conversion of toluene) and ca. 90% acetate plus diacetate (96% conversion), respectively. Attempts have also been made for the past three decades to develop a suitable gas-phase process [15]. One such attempt by Eberson et al. [16] achieved only very low yields of acetoxylated products (∼1% per pass), even with the addition of various promoters (e.g., Au, Bi, Ag–Bi, Au–Bi, etc.) to Pd catalysts. Very recently, Komatsu et al. [17] reported on the gas-phase acetoxylation of toluene over different SiO_2-supported intermetallic Pd compounds like Pd_2Ge, Pd_5Ga_2, Pd_3Pb, Pd_3Bi, etc.; however, only a maximum yield of benzyl acetate of around 7% could be achieved.

A survey of the literature on Pd catalysts for acetoxylation reactions also reveals that various factors, such as (i) addition of a transition metal (e.g., Sb, Bi, Sn, etc.) [7,8,18–20], (ii) particle size of Pd [6], (iii) ratio of Pd to a second metal (Sb, Bi, Sn, etc.) [15,21], and (iv) the nature of the support [6,20] greatly influence the activity and selectivity performance of the catalysts. The incorporation of Sb or Bi to Pd is reported to enhance both the activity and the selectivity of the catalysts in the acetoxylation of butadiene [21–24]. The addition of Sn to Pd is reported to lower the activation energy of the reaction and to serve as a reducing agent in the initial stages of Pd(0) particle formation [8]. Furthermore, it is known that the addition of a second metal will have a synergistic effect in many noble metal-catalysed reactions. The influence of the support on this reaction was mainly investigated on SiO_2, activated carbon, charcoal, and Al_2O_3, but no reports appeared in the literature on the usage of titania (anatase) as an effective support material for the present gas-phase acetoxylation of toluene. Some preliminary results of these investigations were published earlier [25].

From the state of the art it becomes clear that it would be very interesting to increase catalyst performance with respect to gas-phase acetoxylation. In the present investigation, we disclose a first report on the direct synthesis of benzyl acetate in vapour phase in remarkably higher yields compared with the known state with detailed characterisation of the catalysts at different stages of reaction. Furthermore, we report on the influence of Pd loading and particle size on the activity and selectivity behaviour of Pd–Sb–TiO_2 catalysts. The objective of the present investigation is also to further investigate the catalyst performance with time on stream.

2. Experimental

2.1. Catalyst preparation

Two types of TiO_2 (anatase, powder, Kronos; surface area (BET-SA), 315 m^2/g; pore volume, 0.273 cm^3/g)-supported catalysts (monometallic (Pd or Sb) and bimetallic (Pd–Sb)) are prepared by impregnation with $PdCl_2$ (99.8%; Alfa, Karlsruhe, Germany) and/or $SbCl_3$ (99.8%; Alfa). The monometallic samples, such as 8 wt% Sb on TiO_2 (anatase) (8Sb) and 5 wt% Pd on TiO_2 (anatase) (5Pd), were prepared by simple impregnation. The preparation of monometallic 8 wt% Sb–TiO_2 (8Sb) is exactly similar to the first step of bimetallic catalyst preparation described below in more detail. For the preparation of monometallic 5 wt% Pd–TiO_2 (5Pd), 0.42 g of $PdCl_2$ was dissolved in an appropriate amount of distilled water, with a few drops of concentrated HCl, and then warmed up on a water bath at 60 °C for half an hour until it was completely dissolved, and then the pH was adjusted to 4.0 with a few drops of Na_2CO_3 solution. This mixture was then impregnated on TiO_2 (4.75 g) and kept aside for about an hour; after that the excess solvent

was removed by rota vapour and dried in an oven for 16 h at 120 °C.

The bimetallic catalyst preparation involves mainly two steps.

Step 1. We impregnated commercial TiO_2 (anatase) with an aqueous solution of $SbCl_3$ by keeping 8 wt% Sb with respect to the total amount of the catalyst and soaking for 1 h, followed by precipitation with $(NH_4)_2SO_4$ and keeping the temperature at 70 °C for 1 h on a water bath. After cooling to room temperature, the solution was neutralised with ammonia (adjusted to pH 7) and heated on the water bath for another hour. Afterwards the slurry was filtered and dried on a rota-vapour to remove excess water; the resulting solid mass was further dried in an oven at 120 °C for 16 h, followed by calcination at 400 °C for 3 h in air (50 ml/min).

Step 2. The above-mentioned Sb-impregnated TiO_2 sample was again impregnated with the desired amount of acidified aqueous solution of $PdCl_2$ to get the required amount of Pd. The solvent was removed by rota-vapour, and the sample was dried in an oven at 120 °C for 16 h as described elsewhere [26]. The loading of Pd varied in the range of 0.5 to 20 wt% with constant Sb loading (8 wt%). The following anatase-supported samples were prepared: 0.5 wt% Pd (0.5Pd8Sb), 2 wt% Pd (2Pd8Sb), 5 wt% Pd (5Pd8Sb), 8 wt% Pd (8Pd8Sb), 10 wt% Pd (10Pd8Sb), 12 wt% Pd (12Pd8Sb), 15 wt% Pd (15Pd8Sb), and 20 wt% Pd (20Pd8Sb). All used catalysts have the same denotation, but "u" is added at the end (e.g., 0.5Pd8Sb(u)).

2.2. Characterisation of catalysts

The surface areas (BET-SA) and pore size distribution of the catalysts were determined on a Gemini III-2375 (Micromeritics, USA) by N_2-physisorption at −196 °C. Before the measurements, the known amount of catalyst was evacuated for 2 h at 150 °C to remove physically adsorbed water.

The X-ray diffraction (XRD) patterns of the activated samples (300 °C/2 h/air) were obtained with an X-ray diffractometer STADI-P (Stoe, Darmstadt, Germany) and Ni-filtered Cu-K_α radiation ($\lambda = 1.5418$ Å). The samples were analysed after deposition on a quartz monocrystal sample holder supplied by Stoe. We identified the crystalline phases by referring to the ASTM data files.

We prepared samples for transmission electron microscopy (TEM) studies by depositing the sample on a copper grid (300 mesh) coated with carbon film (Lacey). The TEM analyses were carried out with a Philips CM-20 (twin) at 200 kV with EDAX PV9900 (energy dispersive X-ray spectroscopy (EDX)).

The X-ray photoelectron spectroscopic (XPS) measurements were done with an ESCALAB 220iXL. Al-K_α radiation was used to obtain the XP spectra. The spectra were referred to the Ti $2p_{3/2}$ peak of TiO_2 at 458.8 eV. The binding-energy scale was calibrated with pure and clean Cu, Ag, and Au samples. For quantitative analysis after Shirley background subtraction, the peaks were fitted with Gaussian–Lorentz curves. The obtained peak areas were divided by the element-specific Scofield factor and the analysator-specific transmission function to get the composition in the near-surface region.

ICP optical emission spectroscopy (Optima 3000XL; Perkin-Elmer), with a microwave pressure digestion (MDS 200; CEM) with hydrofluoric acid and aquaregia at 9 bar, was used to analyse the chemical composition of fresh and spent catalysts. All samples were analysed twice, so the results are average values.

2.3. Carbon analysis

Carbon analysis was done with a CHN analyser. The samples were packed into lightweight containers of oxydisable metal like Sn and dropped into a vertical quartz tube, heated to 1050 °C, through which a constant flow of helium is maintained. When the sample is introduced, the helium stream is temporarily enriched with pure oxygen. Flash combustion takes place, primed by the oxidation of the container. The exothermic oxidation of Sn raises the temperatures to nearly 1700 °C, at which point a complete combustion of the sample takes place. The resulting combustion products pass through oxidation reagents (WO_3) to produce carbon dioxide, water, and nitrogen from the elemental carbon, hydrogen, and nitrogen (also nitrogen oxides). These gases are then passed over copper to remove excess oxygen and reduce the nitrogen oxides to elemental nitrogen. Helium is used as the carrier gas. The gas from the combustion reactor is introduced into the chromatographic column (PORAPAK QS as a stationary phase), which is heated to about 190 °C. The individual components are then separated; eluted in the order N_2, CO_2, H_2O; and then measured with a thermal conductivity detector (TCD).

2.4. Catalytic measurements

Acetoxylation runs were performed in a continuous fixed-bed, vertical and tubular on-line, micro-catalytic steel reactor (length 112 mm; i.d. 6 mm). The reaction gases, like synthetic air (20.5% O_2 in N_2) as the oxygen source and argon (99.999%) used as the diluent gas, were supplied from commercially available compressed gas cylinders and used without further purification. The flow rates of these gases were measured with mass flow controllers. About 1 ml (ca. 0.8 g) of catalyst particles (0.425–0.6 mm size) is loaded into the reactor and activated in an air flow of 27 ml/min at 300 °C for 2 h before each activity measurement. The organic feed mixture of toluene (Aldrich; purity 99.5%) and acetic acid (Fluka; purity 99.5%) was pumped to the reactor with a HPLC pump (Shimadzu LC 9A). The liquid reactant mixture was vapourised before it entered the reactor in a preheating zone on the top of the reactor. The molar ratios of the reactants, toluene/acetic acid/oxygen/inert gas, were 1:4:3:16. The reactor was heated to reaction temperature in an Ar stream. After it reached reaction temperature,

a mixture of air, argon, and vapourised liquid substrates was introduced, and the reaction was carried out at a temperature of 210 °C and a pressure of 2 bar. The product stream was analysed on line by gas chromatography (GC, HP-5890) with a HP-5 capillary column (50 m × 0.32 mm) and a FID detector. The column outlet was connected to a methaniser (30% Ni–SiO_2 catalyst), which converts all of the carbon-containing products, including CO and CO_2, into methane.

The homemade methaniser consisted of a stainless-steel tube (length 60 mm; i.d. 4 mm) was used for the present analysis. The end of the GC column and the hydrogen supply line for the FID formed the inlets of the methaniser.

The methaniser was packed with 500 mg of a 30% Ni–SiO_2 catalyst and placed at the end of the column so that all of the products could pass through the methaniser after their separation in the column. During analysis, the methaniser was heated to 375 °C. When the column effluent was mixed with the FID hydrogen supply and passed through the methaniser, all compounds were converted into methane. Factors such as catalyst temperature and hydrogen flow normally affect the efficiency of the methaniser. Therefore, optimised levels of these two parameters are used for better conversion efficiency and proper peak symmetry. The conversion efficiency of the methaniser is also determined by analysis of a test sample containing known concentrations of carbon dioxide, carbon monoxide, and methane (e.g., 1% CO_2, 1% CO, 1% CH_4 in argon), which is injected into a Poraplot Q column. It is confirmed that under optimised operating conditions the methaniser is observed to exhibit a conversion efficiency of almost 100%. In other words, the obtained areas for the calibration gases and their ratios confirmed the completeness of hydrogenolysis at 375 °C. It is also found that the hydrogenolysis of the gaseous products did not affect the GC separation quality. Additionally, periodic verification of the efficiency and stability of the methaniser are usually checked from time to time.

As described above, the methaniser converts each compound, leaving the GC column to methane. This allows quantitative detection of all of the volatile compounds as methane, which simplifies the quantitative analysis. To calculate the composition of the product gas, the GC areas of the methanised compounds need only be divided by the individual number of carbon atoms to obtain their molar ratios. Flow rates can then be easily calculated from the known feed rates of the substrates:

Carbon balance: Carbon in = Carbon out.

Separate experiments have shown that the total areas using the methaniser were not influenced by the conversion levels in the range from <1 to over 90%. This confirms the correct functioning of the methaniser. In addition, the amount of carbon fed into the reactor (at 0% conversion during blank tests) is found to be comparable to the amount of carbon leaving the reactor, even at high conversions (within the error margin levels of GC).

Coking has been detected in all of the deactivated catalysts after several hours of catalytic runs. The coking rate, estimated by the ratio between carbon content and the reaction time, was in the range of 1.85×10^{-4} to 5.27×10^{-4} $mol_{carbon}/(h\,g_{cat})$, and the conversion rates were found to be in the range of 0.99 to 5.61 $mol_{toluene}/(h\,g_{cat})$. In a comparison of coke and conversion rates, the influence of coking on the carbon balance appears to be very low.

3. Results and discussion

3.1. Catalyst characterisation

3.1.1. BET surface areas and pore size distribution

BET-SA and pore volumes of the synthesised monometallic and bimetallic samples with various Pd loadings are listed in Table 1. It is clear from the table that monometallic samples exhibited higher surface areas compared with bimetallic catalysts. The surface areas and pore volumes of the bimetallic catalysts are observed to decrease significantly (from 161 to 42 m^2/g and 0.215 to 0.055 cm^3/g, respectively) with increasing Pd loading. This can be attributed to the filling of the small pores and to narrowing of the diameter of the larger pores as a result of the deposition of Pd and/or Sb on the porous surface of the support.

Uncalcined pure titania support exhibits a bimodal pore volume distribution (Fig. 1a). The major contribution of pores to total pore volume occurs mainly in the range of 25–35 Å, as shown in Fig. 1a. In contrast, all of the fresh catalysts reveal a unimodal pore volume distribution with dominant pore diameter at around 30 Å; this supports the assumption of pore filling. The pore volume in this region is observed to decrease continuously with increasing Pd loading. The used catalysts also exhibit unimodal pore volume distribution with a dominant pore diameter around 30 Å similar to that of fresh samples. Nevertheless, the decreasing trend in BET-SA and pore volumes of the used catalysts is found to be more or less similar to that of fresh catalysts (Figs. 1a and b).

Table 1
BET-SA and pore volumes of the support used, monometallic and bimetallic catalysts with different Pd loadings

Sample	BET-SA (m^2/g)	Pore volume (cm^3/g)
Pure TiO_2	315	0.273
8Sb	181	0.228
5Pd	173	0.185
0.5Pd8Sb	161	0.215
2Pd8Sb	156	0.209
5Pd8Sb	127	0.172
10Pd8Sb	78	0.127
15Pd8Sb	55	0.090
20Pd8Sb	42	0.055

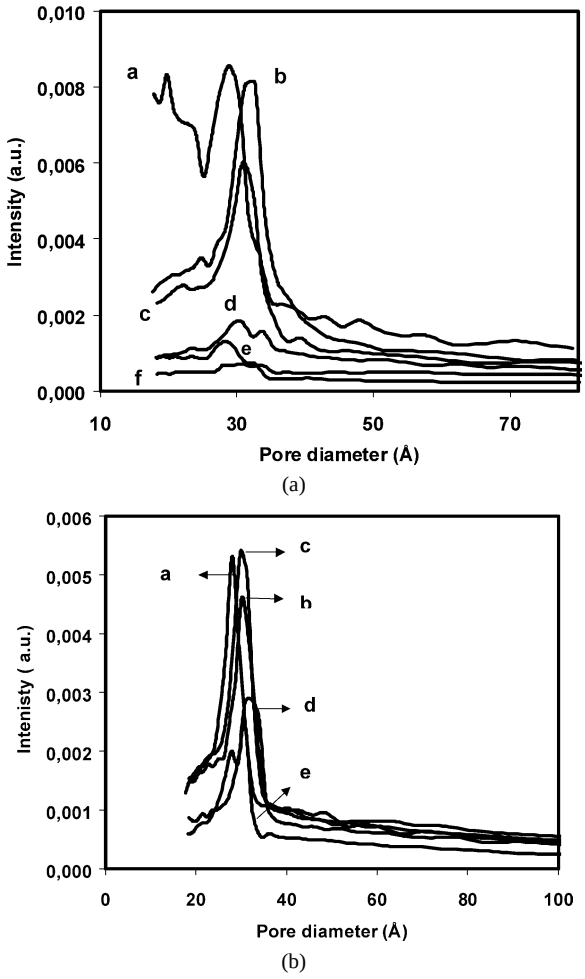

Fig. 1. Pore volume distribution of the fresh (a) Pd–Sb–TiO_2 catalysts with different Pd loadings (a, pure support; b, 0.5Pd8Sb; c, 5Pd8Sb; d, 10Pd8Sb; e, 15Pd8Sb; f, 20Pd8Sb) and used (b) Pd–Sb–TiO_2 catalysts with different Pd loadings (a, 0.5Pd8Sb; b, 5Pd8Sb(u); c, 10Pd8Sb(u); d, 15Pd8Sb(u); e, 20Pd8Sb(u)).

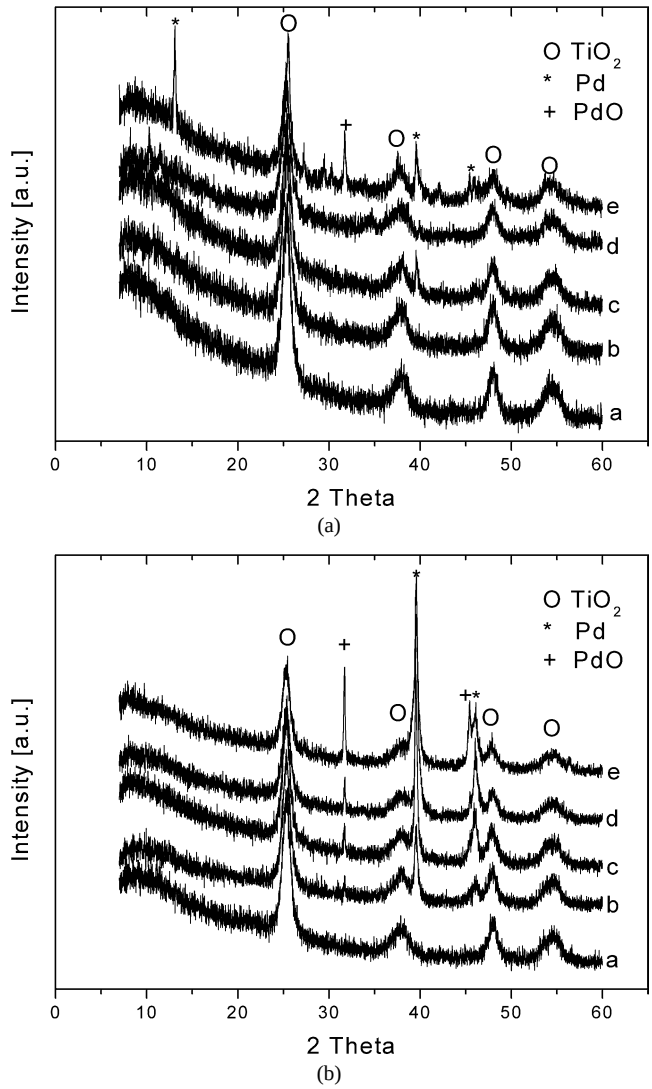

Fig. 2. XRD patterns of fresh (a) Pd–Sb–TiO_2 catalysts with different Pd loadings (a, 0.5Pd8Sb; b, 5Pd8Sb; c, 10Pd8Sb; d, 15Pd8Sb; e, 20Pd8Sb) and used (b) Pd–Sb–TiO_2 catalysts with different Pd loadings (a, 0.5Pd8Sb(u); b, 5Pd8Sb(u); c, 10Pd8Sb(u); d, 15Pd8Sb(u); e, 20Pd8Sb(u)).

3.1.2. X-ray diffraction

The XRD patterns of the fresh activated catalysts (the catalysts were activated as described above) and used catalysts are displayed in Figs. 2a and 2b. The fresh activated catalysts with lower Pd content (up to sample 10Pd8Sb) reveal only reflections that correspond to TiO_2 (anatase) (ASTM card no. 86-1157). However, the samples with a higher proportion of Pd (above 10 wt% Pd) show the presence of both Pd and PdO phases in addition to TiO_2. The XRD patterns of used catalysts are found to be different from those of fresh catalysts, and some of them show a very intense Pd peak, which is indicative for strong sintering. This observation lent good support to the observations made by TEM that the catalysts underwent drastic changes during the course of the reaction as described below. The Pd and PdO phases can clearly be seen in the used catalysts, and the intensity of the reflections that correspond to these phases is increasing with increasing Pd content of the catalysts. In the present study we did not find any crystalline intermetallic phases between Pd-Sb proportions, which are well known from the literature [17,22]. The appearance of oxidised surface Sb species as detected from XPS ruled out the possibility of the formation of intermetallic compounds. Other probable reasons for the absence of intermetallic compounds might also be a different method of preparation and conditioning of the catalysts like calcination, pretreatment/activation temperature, gas atmosphere, etc.

3.1.3. Transmission electron microscopy

Fig. 3 contains a set of TEM images of various fresh Pd–Sb–TiO_2 samples. In the case of sample 0.5Pd8Sb (a) it was difficult to determine the Pd particle size. But with increasing Pd loading up to 10 wt%, free Pd particles can be seen, and their size varied in the range from 1 to 10 nm. The particle size was dramatically increased to 20 nm with further increasing Pd content up to 20 wt% (20Pd8Sb (d)).

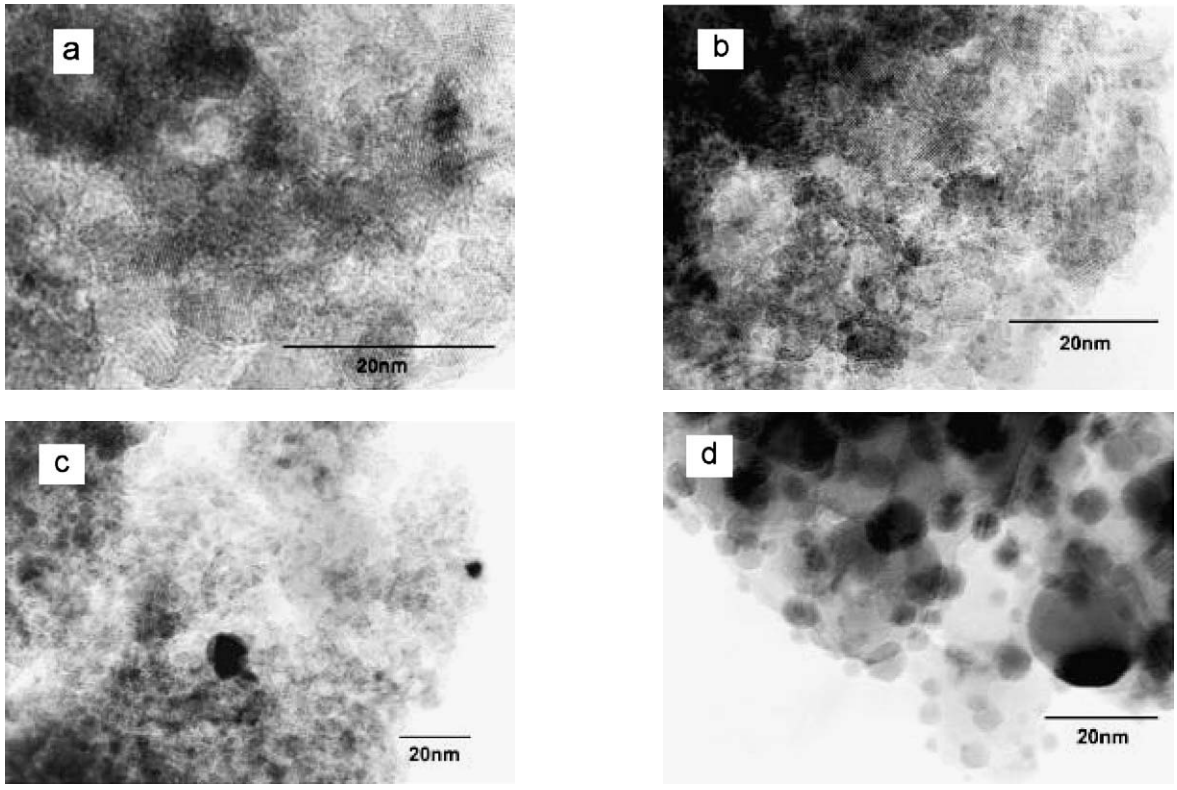

Fig. 3. Electron micrographs of fresh Pd–Sb–TiO_2 catalysts with different Pd loadings (a, 0.5Pd8Sb; b, 5Pd8Sb; c, 10Pd8Sb; d, 20Pd8Sb).

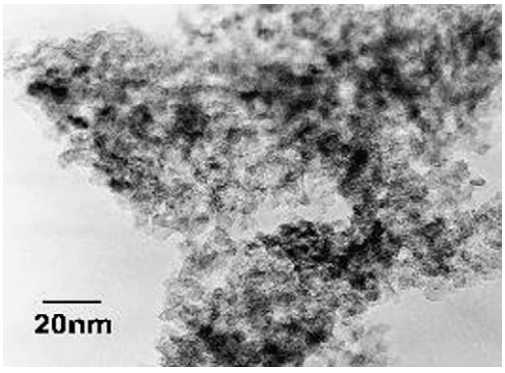

Fig. 4. Electron micrograph of Sb-impregnated titania sample (8Sb).

The particle size of the fresh catalysts reveals a narrow size distribution, and the morphology of Pd-containing particles is spherical. Chlorine was detected in the fresh catalysts by EDX analysis, and the existence of $PdCl_x$ particles seems to be likely, because calcination was not performed after impregnation of $PdCl_2$ during catalyst preparation. Therefore, it is assumed that Pd was present in its precursor state as $PdCl_2$ or $PdCl_x$ ($x = 2$–4) [3] before activation of the catalysts. Chloride analysis by ICP also lent good support to this observation. Antimony was found to cover almost the whole surface of titania, and there was no indication of separated Sb particles (Fig. 4).

It is noteworthy that the particle size of Pd is observed to increase drastically in the used catalysts compared with the corresponding fresh samples (Fig. 5a). Catalyst 0.5Pd8Sb(u) (image (a)) shows a particle size up to 28 nm with spherical shape; for 5Pd8Sb(u) (image (b)) it was observed to increase to 75 nm with a high degree of agglomeration, and for 10Pd8Sb(u) (image (c)) and 20Pd8Sb(u) (image (d)) again the particle size increases even up to 100 nm.

This growth in Pd particle size is possible at two different stages: either during the activation of the catalyst or during the course of reaction. To clarify this aspect both activated and used catalysts were analysed by TEM, and this confirmed that the significant growth in the size of Pd particles is more pronounced during the course of the reaction (Fig. 5a (image c)) rather than in the activation step (Fig. 5b), as expected. Nevertheless, the chloride that we observed in the fresh catalysts was found to be almost removed in the activation step.

The titania is found to be crystalline, as indicated by TEM and XRD analysis. Shen et al. [27] reported from their TEM analysis on TiO_2-supported Pd catalysts with different Pd loadings that Pd particles are hemispherical in shape with a narrow distribution of particles 4–20 nm in size, which are fixed on the well-developed planes of TiO_2. As a result of such matching, the authors suggested that the support structure could stabilise Pd particles. The TEM analysis of supported Pd catalysts by Lyubovsky et al. [28] revealed that the Pd particle size increases considerably after the reaction. They have also observed that most of the particles are round and some are triangular, with sizes ranging from 200 to 300 nm in the used catalysts. This growth in particle size

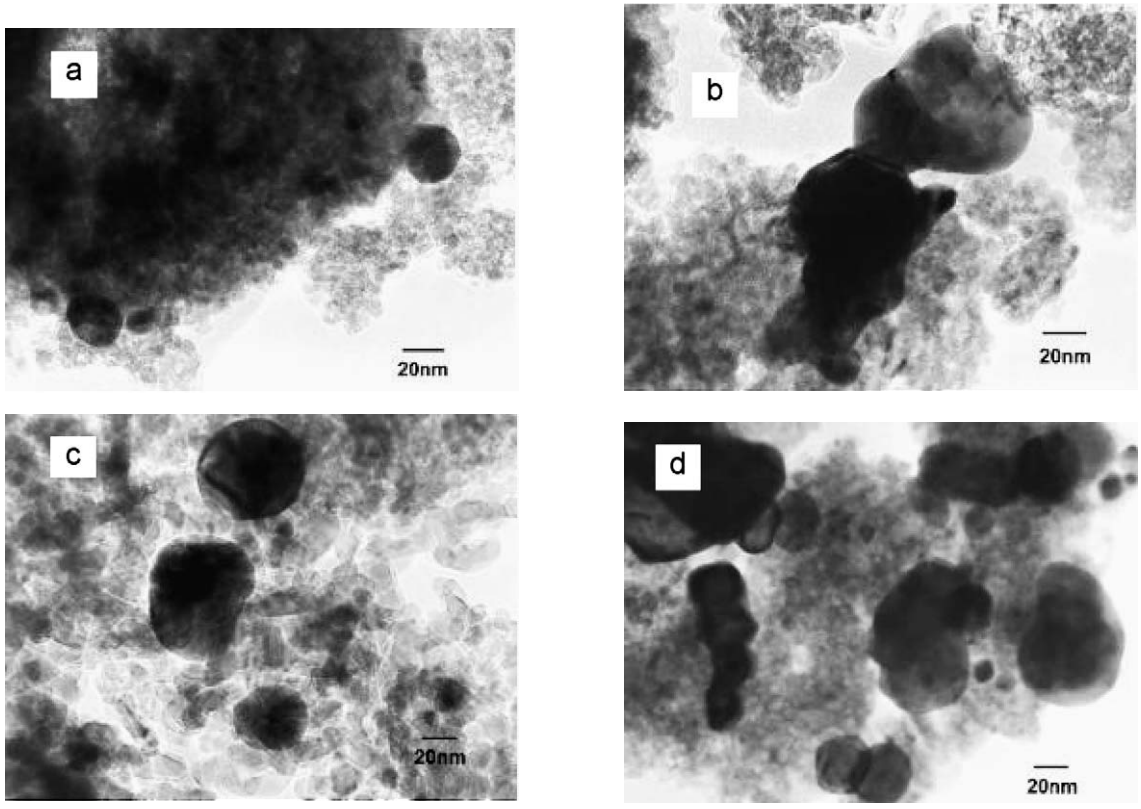

(a)

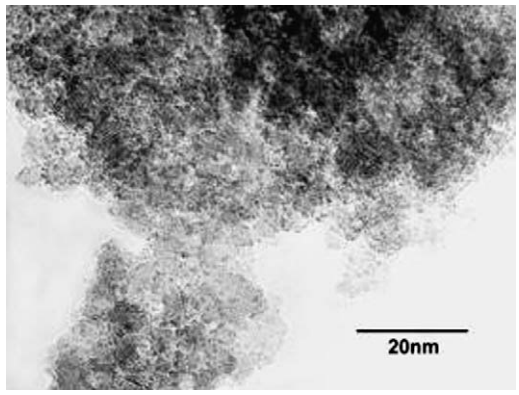

(b)

Fig. 5. Electron micrographs of (a) used Pd–Sb–TiO_2 catalysts with different Pd loadings (a, 0.5Pd8Sb(u); b, 5Pd8Sb(u); c, 10Pd8Sb(u); d, 20Pd8Sb(u)) and (b) 10Pd8Sb activated sample.

after reaction is attributed to the restructuring of metal particles during the course of the reaction.

3.1.4. X-ray photoelectron spectroscopy

The spectra shown in Fig. 6 are the normalised XP spectra after Shirley background subtraction of some fresh and used Pd–Sb–TiO_2 catalysts with different Pd loadings. It is clear that the catalytic reaction leads to a shift of the Pd 3*d* spectra for the used samples to lower binding energies (BE). In the fresh catalysts two components can be observed for the higher Pd loadings. The Pd 3*d* peaks of the fresh 2Pd8Sb sample are broad, which might be a hint of more than one component at this sample. For the used catalysts 2Pd8Sb(u) and 20Pd8Sb(u) only one reduced state could be observed, whereas in the case of 10Pd8Sb(u) two components can clearly be seen.

3.1.5. Variation of bulk to surface Pd/Ti ratios in fresh and used Pd–Sb–TiO_2 catalysts with different Pd loadings

Fig. 7 shows the correlation between the Pd/Ti ratios in the near-surface region obtained with XPS from the corresponding bulk ratio measured with ICP. As can easily be seen, the Pd/Ti ratio of the near-surface region is a continuous function of the bulk ratio from the fresh and used catalysts. At lower Pd loadings up to 2 wt% (0.5Pd8Sb, 2Pd8Sb), no significant differences between the bulk and near-surface

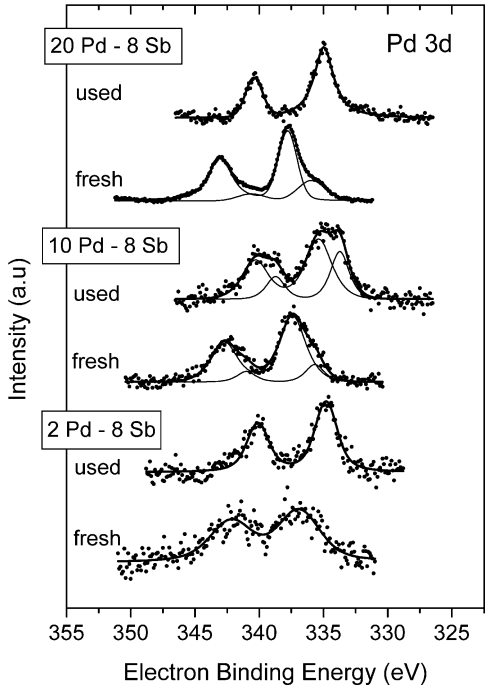

Fig. 6. Normalized XP spectra of the Pd 3*d* state after Shirley background subtraction of the fresh and used Pd–Sb–TiO_2 catalysts with different Pd loadings.

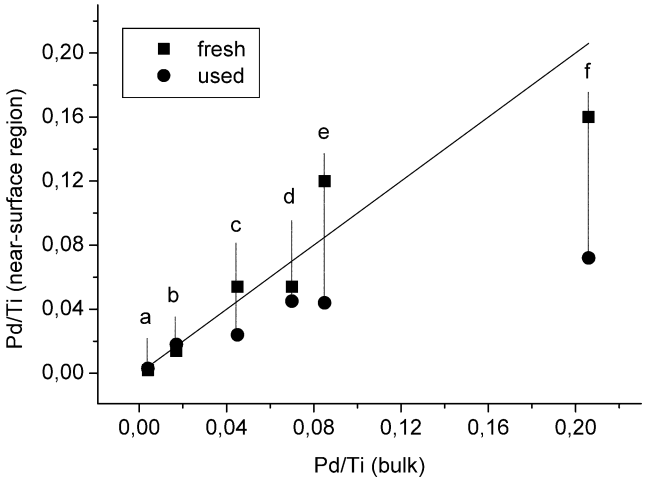

Fig. 7. Variation of bulk to surface Pd/Ti ratio in fresh and used Pd–Sb–TiO_2 catalysts with different Pd loadings (a, 0.5Pd8Sb; b, 2Pd8Sb; c, 5Pd8Sb; d, 8Pd8Sb; e, 10Pd8Sb; f, 20Pd8Sb).

region values are found. The measured BET-SA for these samples, which was relatively high, indicates a small size of TiO_2 particles for which XPS can be regarded more or less as the bulk method. At higher Pd loading (5, 8, 10 wt%) the Pd/Ti ratios for the fresh catalysts are observed to be above the bulk values. This might be explained by a small enrichment of Pd in the surface region of the particles. For the highest Pd loading with 20 wt%, the near-surface Pd/Ti ratios obtained with XPS are significantly lower than the bulk values. This is a hint of an agglomeration of the Pd particles at such high Pd loading. The significantly lower values

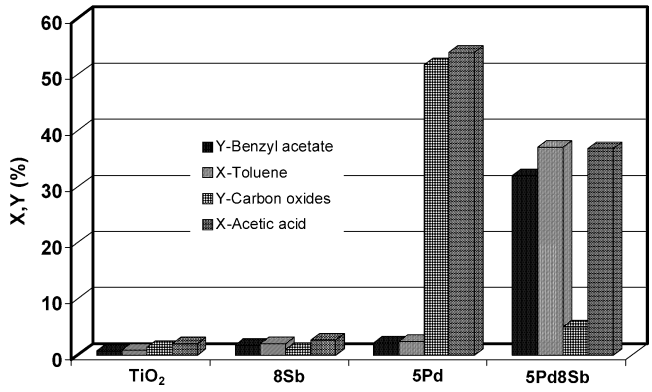

Fig. 8. Acetoxylation runs on pure titania, 8Sb, 5Pd and, 5Pd8Sb samples (molar ratio of toluene:acetic acid:oxygen (air):argon = 1:4:3(15):16, $T = 210\,^{\circ}\mathrm{C}$, GHSV (STP) = 2688 h^{-1}, $\tau = 1,34$ s); X, conversion; Y, yield.

obtained for the used catalyst might point to an agglomeration of larger Pd particles, or it may be due to considerable coke deposition during the reaction. The growth of the Pd particles is well indicated by TEM, which is support by XPS findings.

3.2. Catalytic activity

3.2.1. Synergistic effect of Pd and SbO_x

We have carried out a set of experiments under identical reaction conditions with pure TiO_2 support, monometallic 8Sb and 5Pd samples, and bimetallic 5Pd8Sb to find out the individual roles of Pd and Sb in catalytic performance. The pure titania support is found to be totally inactive (Fig. 8). Furthermore, the catalysts in which Pd and Sb are present alone are found to be almost inactive, giving significantly poor acetoxylation performance. 5Pd catalyst seems to mainly burn acetic acid into carbon oxides (up to 50% CO_x at a toluene conversion of ca. 2%). This observation was also further confirmed by separate experiments, which are explained below. However, it is interesting to note that the combination of the two metals (Pd and Sb) exhibited very high catalytic performance, giving 37% conversion of toluene with a benzyl acetate yield of 32%. The presence of Sb appears to markedly suppress the oxidative decomposition of acetic acid and directs the reaction in a more selective route. In addition, Sb seems to modify significantly the redox properties; however, the precise role of the promoter is still a matter of discussion.

3.2.2. Source of CO_x formation

To find out the origin of formation of CO_x whether from toluene or from acetic acid, we have carried out another set of experiments under identical reaction conditions over 5Pd8Sb catalyst. In the first case, we have performed tests only by feeding toluene (i.e., in the absence of acetic acid) and measured the amount of CO_x formed. In the second case we excluded toluene and fed only acetic acid, and the for-

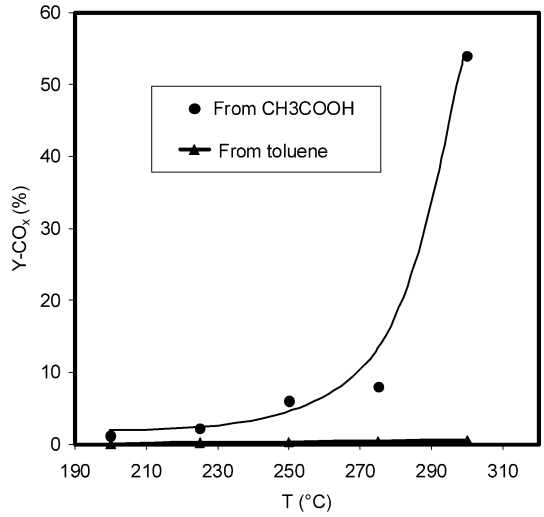

Fig. 9. Confirmatory tests over 5Pd8Sb catalyst for the formation of CO_x either from toluene or acetic acid (Y, yield).

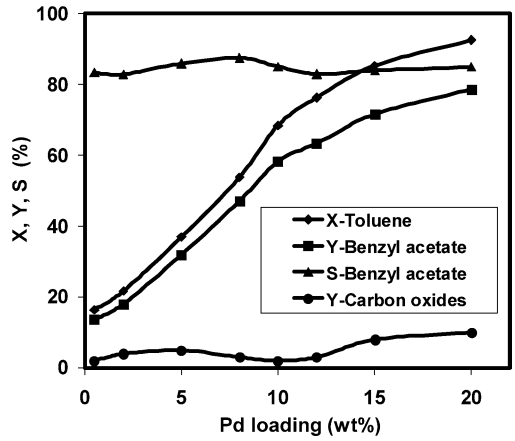

Fig. 10. Influence of Pd loading on acetoxylation of toluene to benzyl acetate over Pd–Sb–TiO_2 catalysts (molar ratio of toluene:acetic acid:oxygen (air):argon = 1:4:3(15):16, T = 210 °C, GHSV (STP) = 2688 h^{-1}, $\tau = 1, 34$ s); X, conversion; Y, yield; S, selectivity.

mation of CO_x was again measured. Fig. 9 summarises the results.

It is surprising that the formation of CO_x from toluene is almost negligible even at 300 °C, whereas the formation of CO_x from acetic acid is found to be remarkably significant. Both the conversion of acetic acid and the yield of CO_x are increased continuously from 1.2 to 54% with increasing temperature from 200 to 300 °C. However, the formation of CO_x from toluene in every case is less than 0.5%, regardless of temperature. These observations clearly indicated that the formation of CO_x occurs mainly from the oxidative decomposition of acetic acid but not from toluene.

3.2.3. *Influence of Pd loading on acetoxylation of toluene*

The influence of Pd loading on acetoxylation activity over Pd–Sb–TiO_2 (anatase) catalysts is presented in Fig. 10. It is evident from the figure that the Pd loading has a promotional effect on the conversion of toluene, which has increased substantially from 16 to 92% with increasing Pd loading. At very low Pd loading, the conversion and yield of benzyl acetate were found to be very low, about 16 and 14%, respectively. It is apparent from the results that there is a strong dependence of catalytic activity on time on stream. For better comparison of the activity of various catalysts with different Pd loadings, the steady-state activity (maximum activity) is considered instead of the same reaction time. This is done because it is not appropriate to take the same time of reaction for all of the catalysts, as the activity depends on Pd particle size, which is found to change with time in a way similar to that of activity. Higher Pd loading catalysts containing larger Pd particles exhibit relatively higher activity in less time compared with lower loading catalysts that contain smaller Pd particles. Achieving this steady condition (though it is retained for a short period of time, 2–4 h) differs from catalyst to catalyst, depending on Pd loading, because we need a particular size of Pd particles to obtain better activity. The lowest Pd loading catalyst (0.5Pd8Sb) took about 15 h to exhibit maximum activity, whereas the highest Pd loading catalyst (20Pd8Sb) took only 7 h to display maximum activity.

The other by-products formed from this reaction are benzaldehyde and total oxidation products (CO_x). The yields of benzaldehyde vary in the range from 3 to 13%, and CO_x is found to be between 2 and 10%. However, one should assume that the formation of CO_x is occurring mainly from the oxidative decomposition of acetic acid rather than toluene, as discussed above.

The high conversions and high yields at higher Pd loading are probably due to an increase in Pd particle size. Neri et al. [29] have observed that both the catalytic activity and selectivity of Pd–C catalysts in the hydrogenation of 2,4-dinitrotoluene also increased with increase in Pd particle size. According to Suh et al. [30], the less dispersed supported Pd catalysts are the most active catalysts, and they attributed the increase in specific activity of Pd–C catalysts also to larger Pd metal particles. A similar correlation was also reported for catalytic oxidation of methane, a reaction that depends on Pd loading [31]. A similar effect was also observed by Benedetti et al. [32] in the hydrogenation of 2,4-dinitrotoluene over Pd–SiO_2 catalysts. Our results on the influence of Pd particle size on the activity and selectivity behaviour of the catalysts are in good agreement with those reported above in the literature for various catalytic reactions over supported Pd catalysts.

3.2.4. *Time-on-stream studies over 20Pd8Sb catalyst*

Fig. 11 clearly demonstrates the changes in catalytic performance with time on stream over 20Pd8Sb. For better comparison of the activity of various catalysts with different Pd loadings, the steady-state activity is considered instead of same reaction times. It is interesting to note that all of the tested catalysts are found to attain steady-state conditions after several hours of operation. In other words, the catalysts display a very low initial activity, which is observed to in-

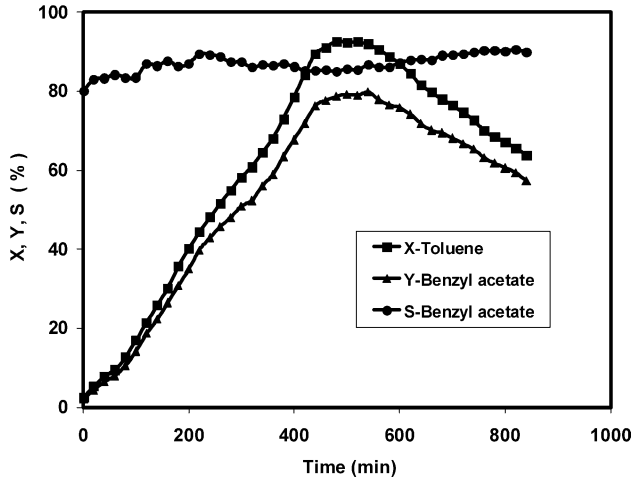

Fig. 11. Time-on-stream behaviour of 20Pd8Sb catalyst as function of yield, conversion and selectivity (molar ratio of toluene:acetic acid:oxygen (air):argon = 1:4:3(15):16, $T = 210\,^{\circ}\mathrm{C}$, GHSV (STP) = 2688 h^{-1}, $\tau = 1.34$ s); X, conversion; Y, yield; S, selectivity.

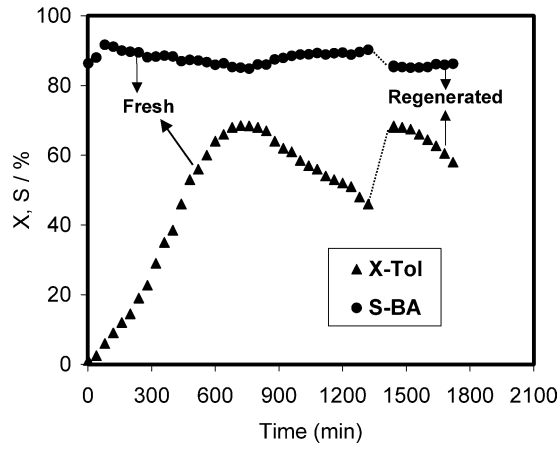

Fig. 12. Comparison of performance of fresh and regenerated 10Pd8Sb catalyst (molar ratio of toluene:acetic acid:oxygen (air):argon = 1:4:3(15):16, $T = 210\,^{\circ}\mathrm{C}$, GHSV (STP) = 2688 h^{-1}, $\tau = 1.34$ s); X, conversion; S, selectivity.

crease considerably with time. Normally, the catalysts are found to exhibit maximum activity after several hours of operation. This fact shows that the catalysts need a certain time for the growth of Pd particles to a critical size, which appears to be essential for obtaining maximum activity. These ideas are well supported by our TEM analysis results for fresh, maximum active and used catalysts. It has also been found from characterisation results that the higher activity is always associated with the catalysts that contain larger Pd particles, which are formed during the course of reaction only after a certain period of time. However, the increase in Pd particle size alone may not be responsible for the better performance of catalysts. Other alternative possibilities for better performance with increased Pd loading might also be preferential exposure of specific crystallographic phases, formation of new active centres, enhanced metal support interaction, and so on. However, our characterisation results did not give any supporting evidence for such hypotheses.

The major problem with these catalysts is deactivation due to considerable amounts of coke deposits after several hours of operation. The amount of coke estimated for 20Pd8Sb(u) was found to be 7.3 wt% (after 14 h of time-on-stream studies). No significant difference in the size of Pd particles between highly active and deactivated catalysts can be seen from TEM. The only difference between these two samples is the amount of coke deposits. This result indicates that the deactivation is due mainly to coke deposition rather than the further agglomeration of Pd particles, which seemed to be favourable for better performance. However, the catalysts can be effectively regenerated in air (250 °C/2 h) to restore immediately the maximum activity that has been lost because of coke deposits. The regenerated catalysts showed consistent performance for more cycles because of the effective removal of coke from the catalyst surface.

3.2.5. Comparison of time-on-stream behaviour of fresh and regenerated 10Pd8Sb catalyst

Fig. 12 demonstrates the time-on-stream performance of fresh and regenerated 10Pd8Sb catalyst. It is quite obvious from the figure that the deactivated catalyst after regeneration in air immediately restores its maximum activity and selectivity as that of fresh catalyst. It is also indicated that there are no significant changes between fresh and regenerated catalysts, particularly in the tendency of change of activity and selectivity behaviour with time on stream. Both the fresh and regenerated catalysts exhibited conversion of toluene as high as 68% and benzyl acetate selectivity of ca. 85%. The fresh catalyst is observed to exhibit very low initial activity (ca. 2%), which increases further to a maximum of 68% after around 11 h, remains stable for another 3 h, and then begins to decline with time, 46% at 22 h. At this stage, the reaction is deliberately stopped, and the catalyst is regenerated in air at 250 °C for 2 h, and then the reaction is continued under identical conditions in order to compare its performance with that of the fresh catalyst. The dotted line in Fig. 12 indicates the duration of regeneration time (2 h). It is noteworthy that the tendency of catalytic performance is observed to be similar in all of the catalysts regardless of Pd loading. In addition, a comparison of the activity and selectivity behaviour of fresh and regenerated Pd–Sb–TiO_2 catalysts with different Pd loadings is presented in Table 2. It is very clear that the regenerated catalysts consistently displayed a performance comparable to that of fresh catalysts.

After fresh and used catalysts have been characterised by various techniques, the changes that have been observed are (i) an increase in crystallinity of the samples without any change in the phase composition (i.e., both fresh and used catalysts contain mainly Pd and PdO phases, as seen from XRD), (ii) a significant increase in Pd particle size (from TEM), (iii) a considerable amount of coke deposition in the used catalysts (from carbon analysis), and (iv) loss of both Sb and Pd at the surface (indicated by XPS). But it is not

Table 2
Comparison of toluene acetoxylation activity of fresh and regenerated Pd–Sb–TiO_2 catalysts with different Pd loadings (8 wt% Sb)

Pd (wt%)	Fresh catalysts			Regenerated catalysts		
	X-Tol (%)	*Y*-BA (%)	*S*-BA (%)	*X*-Tol (%)	*Y*-BA (%)	*S*-BA (%)
0.5	16.4	13.7	83.4	16.5	13.8	83.6
2	21.7	18.0	82.9	20.8	17.4	83.4
5	37.0	32.0	86.0	36.0	31.0	86.0
8	53.8	47.1	87.6	53.2	47.0	87.7
10	68.5	58.3	85.1	68.0	58.0	85.3
12	76.4	63.4	83.0	74.9	62.6	83.6
15	85.3	71.6	84.0	84.7	72.0	85.0
20	92.6	78.7	85.0	92.0	78.5	85.3

BA, benzyl acetate; *X*, conversion; *Y*, yield; *S*, selectivity.

very clear that these changes have occurred either during the activation step (300 °C/2 h/air) or during the course of catalytic runs at different reaction times. Keeping these aspects in mind, we have taken 10Pd8Sb as a model catalyst and subjected it to different test runs under identical conditions by varying reaction times and then characterised all of these samples by various techniques. The details of the results for this catalyst subjected to different stages of reaction are discussed in the following section.

3.3. Solid-state properties of 10Pd8Sb at different stages of the reaction

With the above-mentioned aspects in mind, the 10Pd8Sb catalyst, which lies in the middle of the series (i.e., between high and low Pd loading) in addition to displaying appreciably good performance, has been taken as a model catalyst and used to characterise further the changes that occur during different stages of reaction.

This catalyst has exhibited ca. 68% conversion of toluene and 85% selectivity for benzyl acetate (Y(benzyl acetate) = ca. 58%). The reaction is performed to a particular stage, and then the reaction is deliberately stopped, the reactor is cooled, and the catalyst is unloaded and analysed. This is how the catalyst is intentionally subjected to different stages and analysed. Different stages of reaction that were selected in the present study are (i) catalyst activation (300 °C/2 h/air), (ii) when the catalyst becomes half active ($X = 35\%$; i.e., after 6 h of reaction), (iii) maximum activity ($X = 68\%$, i.e., after 11 h of reaction), (iv) after 4 h of deactivation ($X = 57\%$, i.e., after 18 h), (v) after 8 h of deactivation ($X = 46\%$, i.e., after 22 h), (vi) when the sample is regenerated (i.e., the same sample tested for 22 h). Then the samples are analysed by various techniques, such as nitrogen physisorption, TEM, XPS, and XRD for better understanding of these changes and their possible influence on the catalytic performance. All of these changes, observed with various techniques, are discussed in detail in the following sections.

Table 3
BET-SA and pore volumes of the 10Pd8Sb catalyst at different stages of reaction

Sample	BET-SA (m^2/g)	Pore volume (cm^3/g)
Fresh catalyst	78	0.127
Activated	79	0.119
Half active ($X = 35\%$)	88	0.136
Maximum active ($X = 68\%$)	80	0.120
After 4 h of deactivation ($X = 57\%$)	80	0.124
After 8 h of deactivation ($X = 46\%$)	64	0.089
Regenerated ($X = 68\%$)	128	0.159

3.3.1. BET-SA and pore size distribution of 10Pd8Sb catalysts

It is clear from Table 3 that the deactivated sample exhibited the lowest surface area (64 m^2/g) and pore volume (0.089 cm^3/g) due to pore blocking by coke deposits (ca. 6 wt%) and the regenerated catalyst after effective removal of coke displays the highest surface area and pore volume of 128 m^2/g and 0.159 cm^3/g, respectively. Therefore, the surface area has been decreased by about 50% in the deactivated catalyst compared with the regenerated one. The increase in BET-SA of the regenerated sample can be attributed to the removal of coke from the catalyst surface, which caused a weakening of the pores, and the surface structure underwent slight alterations. Moreover, during the regeneration procedure most of the surface Pd is oxidised, which is also observed by XPS. However, there is no appreciable change in the surface areas from the fresh sample to a stage of maximum activity. A slight decrease in surface area of the most active catalyst might be due to a small amount of coke deposition (2.3 wt%) on the catalyst surface at this stage. The amount of coke estimated to be in the deactivated sample, after 22 h of reaction, was about 6 wt%, which is very high.

No significant changes in the pore size distribution of this catalyst at different stages of reaction were noticed, as shown in Fig. 13. These patterns are more or less similar to those of the fresh and used catalysts showing unimodal pore volume distribution. The only difference is in their intensity, which is due to the difference in their surface areas and pore volumes.

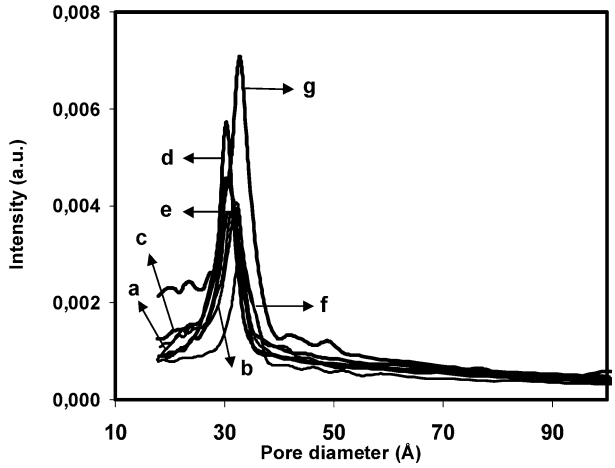

Fig. 13. Pore volume distribution of 10Pd8Sb catalyst at different stages of reaction (a) fresh, (b) activated, (c) half active ($X = 35\%$), (d) maximum active ($X = 68\%$), (e) deactivated after 4 h ($X = 57\%$), (f) deactivated after 8 h ($X = 46\%$), (g) regenerated ($X = 68\%$).

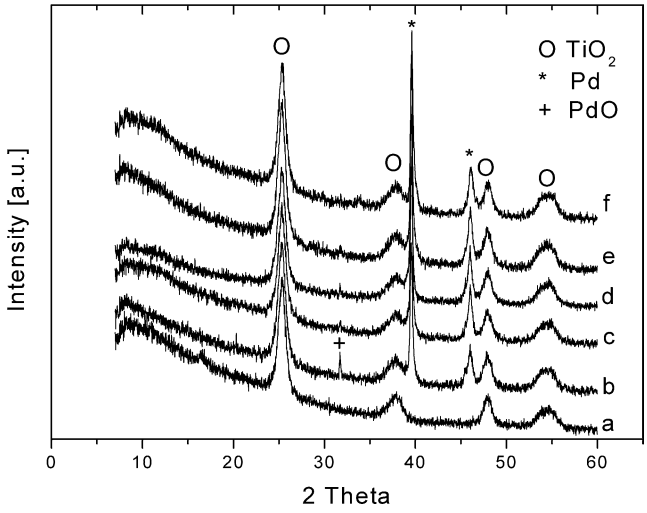

Fig. 14. XRD patterns of 10Pd8Sb catalyst at different stages of reaction (a) activated, (b) half active ($X = 35\%$), (c) maximum active ($X = 68\%$), (d) deactivated after 4 h ($X = 57\%$), (e) deactivated after 8 h ($X = 46\%$), (f) regenerated ($X = 68\%$).

3.3.2. X-ray diffraction of 10Pd8Sb catalysts

From XRD analysis, which is described in Fig. 14, no significant changes in the phase composition of the catalyst are observed at different stages of the reaction. The samples exhibit only Pd and PdO phases in addition to intense reflections that correspond to the support TiO_2 (anatase) phase at every stage of reaction, which are similar to those of fresh and used catalysts.

3.3.3. Transmission electron microscopy of 10Pd8Sb catalysts

Fig. 15 shows a series of TEM images of 10Pd8Sb samples taken at different stages of the reaction as mentioned above. The first image (a) corresponds to an activated sample, which is more or less similar to the fresh catalyst. This result implies that Pd particle growth does not occur during the activation step. The sample contains some larger Pd particles up to 10 nm. However, the range of Pd particles is distributed in the range from 1 to 10 nm. If we watch the image (b), after 6 h of catalytic runs, where the activity reached nearly half (i.e., 35%), the sample contains a mixture of both smaller ($\sim$2 nm) and some larger particles up to 20 nm, indicating growth of Pd particles that started during the course of the reaction. Another interesting point is that the particle size increases continuously until it reaches a maximum (up to ca. 80–100 nm), and then no further increase is observed. Nevertheless, when the catalyst exhibited maximum activity (image c), it also contained larger Pd particles, even up to 100 nm. In addition, at this stage of reaction the particles tend to develop some faceting, a sign of further perfection of crystallisation. The conversion of toluene increased from 35 to 68% with increasing Pd particle size due to further agglomeration. The maximum activity remains constant for about 3 h and starts declining without undergoing any change in the Pd particle size. After 18 h on stream the catalyst, with more or less similar Pd particles, lost about 16% of its activity (from 68 to 57%) (image d). This tendency of decreasing activity is continued further with time on stream. After 22 h of tests, the conversion of toluene is further reduced to 46%, but there is again no change observed in Pd particle size (image e). This fact proves on the one hand that the catalytic performance is strongly dependent on Pd particle size and the larger particles are favourable for better performance of the catalysts, which is in good agreement with the literature [6]. On the other hand, catalyst deactivation is mainly due to coking. The amount of coke deposition is also observed to increase continuously with time on stream, about 5.5% in the catalyst tested for 18 h, and to increase slightly to 5.8% after 22 h of testing, against only 2.3% in the maximum active catalyst. Furthermore, this considerable amount of coke deposition, in turn, affected the surface concentration of both Pd and Sb species, which were analysed by XPS and are discussed below. The regenerated catalyst exhibited activity ($X = 68\%$) similar to that of the maximum active catalyst. The Pd particle size in this regenerated sample (image f) is found to be more or less similar to those of maximum active and deactivated samples. The only difference is the lower amount of coke in the regenerated sample compared with its corresponding deactivated catalyst. This observation indicates that the regeneration process is effective in the removal of coke deposits from the catalyst surface, but it has no effect on Pd particle size.

3.3.4. Electronic structure of Pd showing different surface Pd species in 10Pd8Sb catalysts

XPS analysis showed the presence of three types of Pd species on the surface of this catalyst at different stages of the reaction (Fig. 16). These surface Pd species are (i) the metallic species, called Pd(0); (ii) oxidised Pd components, labelled with Pd (Ox); and (iii) a species with a lower binding energy than Pd(0), denoted as Pd($\delta-$). The standard value of BE for Pd(0) is 335.1 eV [33], and the species show-

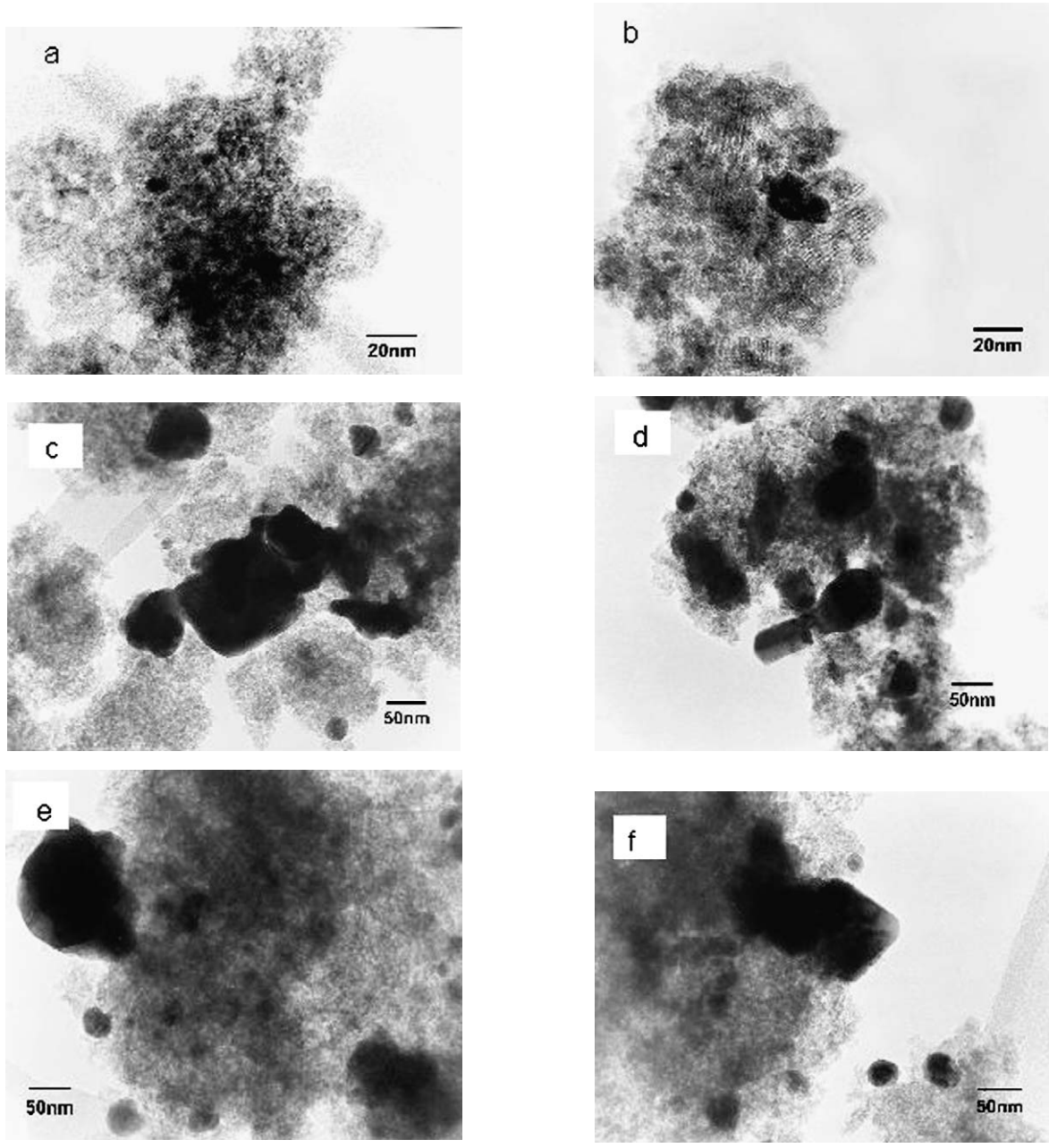

Fig. 15. Electron micrograph of 10Pd8Sb catalyst at different stages of reaction (a) activated, (b) half active ($X = 35\%$), (c) maximum active ($X = 68\%$), (d) deactivated after 4 h ($X = 57\%$), (e) deactivated after 8 h ($X = 46\%$), (f) regenerated ($X = 68\%$).

ing higher BE values than Pd(0) indicate that the Pd is in oxidised form. But it is difficult to assign this species to either Pd(II) or Pd(IV), because no standards for these species are available in the literature and the BE values for these species will change with changing composition. The formation of the third type, the Pd($\delta-$) species, is probably due to the interaction between surface Pd and the deposited coke.

Interestingly, the three species are not present together on the surface of this catalyst at any stage of the reaction. They may also be interconvertible from one species to another during the course of the reaction. However, no such changes in the electronic state of Sb are noticed. The BE values for surface Sb remained more or less constant at around 540 eV, which is between Sb(III) and Sb(V) and indicates that the surface Sb species are oxidised. The exact values of BE for Sb(III) and Sb(V) are Sb(III) = 539.5 eV and Sb(V) = 540.4 eV [34].

3.3.5. Different Pd species on the surface of 10Pd8Sb catalysts

To quantify these three different surface Pd species described above, the next step of the investigation is intended to derive a correlation between the amount of these surface Pd species and catalytic performance. It is evident

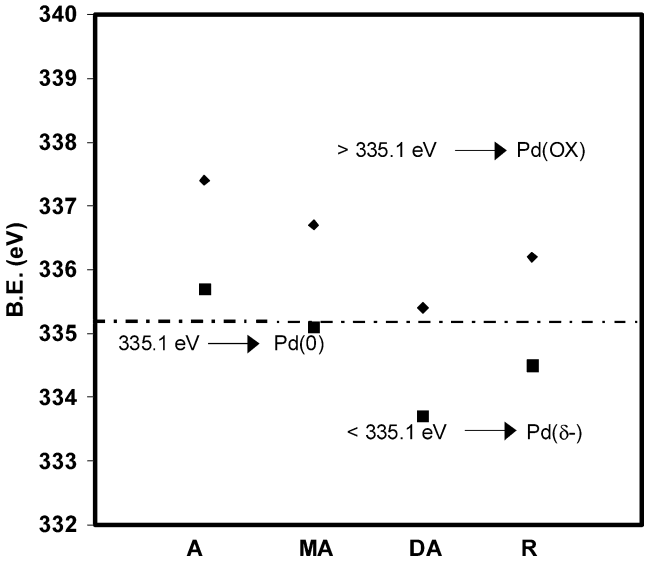

Fig. 16. Electronic structure of Pd showing different surface Pd species in 10Pd8Sb catalyst at different stages of reaction (A, activated; MA, maximum active; DA, deactivated; R, regenerated).

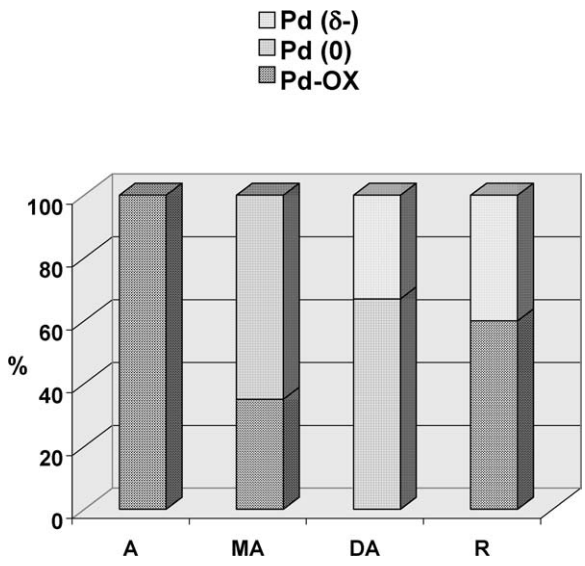

Fig. 17. Different Pd species on the surface of 10Pd8Sb catalyst at different stages of reaction (A, activated; MA, maximum active; DA, deactivated; R, regenerated).

from Fig. 17 that the activated sample, after the treatment at 300 °C/2 h/air, contains exclusively (100%) oxidised surface Pd species, as expected. In the catalyst, when it becomes most active, the surface consists of both metallic Pd (65%) and Pd–OX (35%) species.

It is noteworthy that no Pd-oxidised surface species exist in the deactivated catalyst; instead it contains only Pd(0) and Pd($\delta-$) species. However, the regenerated catalyst, which again displayed maximum activity, contains Pd–OX and Pd($\delta-$) species. It is also worth mentioning that though three different surface species exist in these samples, the three species never present together in any sample at any stage of the reaction. The estimated carbon content of these catalysts

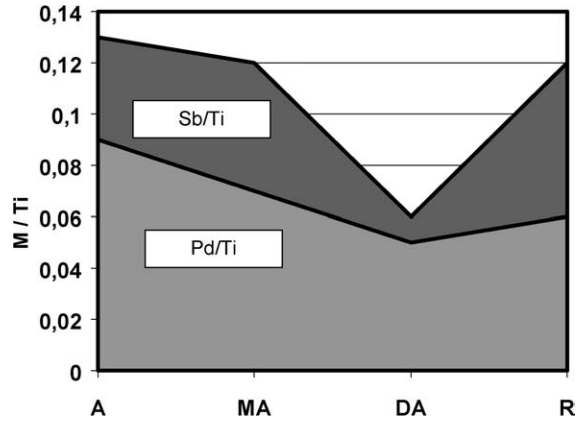

Fig. 18. Variation of bulk to surface Pd/Ti and Sb/Ti ratios in 10Pd8Sb catalyst at different stages of reaction (A, activated; MA, maximum active; DA, deactivated; R, regenerated).

was found to be almost negligible in the case of activated catalyst and to be 2.3 wt% when the catalyst reached maximum activity. The deactivated catalyst exhibited the highest carbon content (5.8 wt%), and the regenerated sample in air for 2 h at 250 °C exhibited the lowest carbon content (ca. 1.7 wt%).

We can conclude from this result that both Pd and PdO are the active species for the reaction, and the formation of Pd($\delta-$) comes from the interaction of Pd with carbon, which is deposited on the surface during the course of the reaction.

3.3.6. Variation of bulk to surface Pd/Ti and Sb/Ti ratios in 10Pd8Sb catalyst at different stages of reaction

To examine the distribution of Pd and Sb in the near-surface region (about 5 to 10 nm depth) in the 10Pd8Sb sample at different stages of reaction, the ratios of Pd/Ti and Sb/Ti were calculated; these are presented in Fig. 18.

The surface concentration profiles of these two components (i.e., Pd and Sb) indicate that both Pd/Ti and Sb/Ti ratios are decreased considerably in the deactivated catalyst. This decrease is undeniably due to coke deposition and particle agglomeration. Nevertheless, this decrease is more pronounced in the case of Sb compared with Pd. The precise reason for this behaviour is not known yet; a preferred deposition of coke on the Sb atom in the presence of Pd(0) can be suggested as the best explanation. However, the regeneration process effectively restored an almost similar surface concentration of Sb and partly increased Pd because of removal of coke from the catalyst surface (see also Fig. 17).

Interestingly, these two ratios (i.e., Pd/Ti and Sb/Ti) are found to be more or less similar in the catalysts with the maximum activity and the regenerated catalyst. This observation also indicates that the presence of Sb at the surface is highly essential for obtaining better performance of the catalyst.

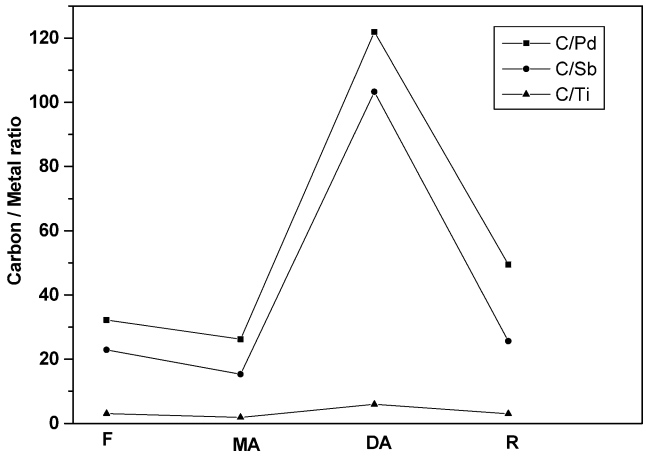

Fig. 19. Variation of carbon to metal ratios (C/Pd, C/Sb, C/Ti) in the near surface region of 10 Pd–Sb–TiO_2 catalyst at different stages of reaction (F, fresh; MA, maximum active; DA, deactivated; R, regenerated).

3.3.7. Variation of carbon/metal ratios (C/Pd, C/Sb, C/Ti) in the near-surface region of 10 Pd–Sb–TiO_2 catalyst at different stages of reaction

As discussed earlier, coke deposition is observed to occur during the reaction and to increase with time on stream, ultimately leading to deactivation. Keeping this aspect in mind, the variations in carbon/metal ratios in the near-surface region were calculated; these are illustrated in Fig. 19. It is evident from the data shown in the figure that the carbon is deposited preferentially on Pd and Sb during the reaction. The deactivation is accompanied by a sudden jump in C/Pd and C/Sb ratios in the near-surface region. Among these three metals, Pd is strongly influenced by coke deposition. The surface ratio of C/Pd is abruptly increased from 32 in the fresh catalyst to 122 in the deactivated catalyst. However, the regeneration process has brought down this C/Pd ratio to around 50 because of effective removal of coke from the surface. A similar tendency is observed for the C/Sb ratio, which is much higher in the deactivated sample (> 100) compared with all other stages of the reaction (ca. 25). On the other hand, coke deposition is found to have no considerable influence on the surface C/Ti ratio, which varies over a very narrow range from 2 to 6 in the catalyst at different stages of the reaction. After the regeneration by oxygen, C/Sb and C/Ti ratios were restored to nearly the same values as earlier (i.e., before deactivation). In contrast, the C/Pd ratio is found to remain at a higher level compared with fresh and maximum active stages of the reaction. This can be explained by a strong interaction between C and Pd. This stable Pd–C interaction could be due to some negatively charged carbon species on the Pd clusters as intermediates of the reaction and a charge transfer from the carbon to the metal atoms. In all cases the main C1*s* peak around 284.5 eV is typical for C–C and C–H bonds. This peak is relatively broad, indicating a high chemical diversity of these states. Another C1*s* peak could be found around 289 eV and can be correlated with carboxyl groups.

4. Conclusions

The monometallic catalysts (i.e., Pd–TiO_2 and Sb–TiO_2) were not found to be active for the acetoxylation of toluene, whereas the combination of both Sb and Pd in Pd–Sb–TiO_2 catalysts markedly enhanced the catalytic activity and reaction selectivity for the desired product (benzyl acetate). The addition of Sb to Pd also significantly suppressed the oxidative decomposition of acetic acid and directed the reaction in more selective route. Furthermore, the presence of Sb seems to modify the redox properties of the catalysts. Pd and PdO are assumed to be the active sites for the acetoxylation of toluene. The larger Pd particles were found to be favourable for obtaining better performance. The loss of Pd and Sb in the near-surface region caused by coke deposition on the catalyst surface is the main reason for the catalyst deactivation. The regeneration step was found to be mainly a cleaning of coke from the surface, which has no influence on particle size and phase composition. Nevertheless, this route is a green process; the catalyst can easily be regenerated and reused for more cycles with consistent performance. Further studies are needed, however, to verify the exact nature of the active sites and identify the probable reaction mechanism.

Acknowledgments

The authors are grateful to Mrs. R. Bienert, Mrs. S. Evert, Mrs. G. Klinger, and Mrs. W. Winkler for experimental assistance.

References

[1] K. Bauer, D. Garbe, H. Surburg, in: W. Gerhartz (Ed.), Ullmann's Encyclopaedia of Industrial Chemistry, vol. A11, VCH, Weinheim, 1988, p. 141.
[2] M. Constantini, L. Krumenacker, Stud. Surf. Sci. Catal. 44 (1989) 159.
[3] O. Takeru, W. Keisuke, US Patent 4,033,999 (1977) (Mitsubishi Chemical Industries, Japan).
[4] D.R. Bryant, J.E. McKeon, B.C. Ream, J. Org. Chem. 33 (1968) 4123.
[5] L. Eberson, L.G. Gomez-Gonzalez, Acta Chem. Scand. 27 (1973) 1249–1255.
[6] E. Benazzi, H. Mimoun, C.J. Cameron, J. Catal. 140 (1993) 311.
[7] S.K. Ivanov, S.K. Tanielyan, Oxidn. Commun. 7 (1984) 69.
[8] E. Benazzi, C.J. Cameron, J. Mol. Catal. 69 (1991) 299.
[9] L. Eberson, L. Jönsson, Acta Chem. Scand. (B) 28 (1974) 771.
[10] G.G. Arzoumanidis, F.C. Rauch, J. Org. Chem. 28 (1973) 4443.
[11] M.I. Vargraftik, V.I. Zagorodnikov, I.I. Moiseev, Kin. Katal. 22 (1981) 951.
[12] P.M. Maitlis, The Organometallic Chemistry of Palladium, vol. 2, Academic Press, New York, London, 1971.
[13] T. Miyake, A. Hattori, M. Hanaya, S. Tokumaru, H. Hamaji, T. Okada, Top. Catal. 13 (2000) 243.
[14] K. Ebitani, K.-M. Choi, T. Mizugaki, K. Kaneda, Langmuir 18 (2002) 1849.
[15] M. Martin, G. Scharfe, W. Swodenik, DE Patent 2,107,913 (1971) (Bayer).
[16] L. Eberson, L. Jönsson, Acta Chem. Scand. (B) 28 (1974) 597.

[17] T. Komatsu, K. Inaba, T. Uezono, A. Onda, T. Yashima, Appl. Catal. 251 (2003) 315.
[18] O. Takeru, W. Keisuke, DE Patent 2,505,749 A1 (1975) (Mitsubishi Chemical Industries, Japan).
[19] M. Wenkin, C. Renard, P. Ruiz, B. Delmon, M. Devillers, in: R.K. Graselli, S.T. Oyama, A.M. Gaffney, J.E. Lyons (Eds.), 3rd World Congress on Oxidation Catalysis, 1997, p. 517.
[20] S.K. Tanielyan, R.L. Augustine, J. Mol. Catal. 90 (1994) 267.
[21] H. Shinohara, Appl. Catal. 10 (1984) 27.
[22] H. Shinohara, Appl. Catal. 14 (1985) 145.
[23] H. Shinohara, Appl. Catal. 30 (1987) 203.
[24] H. Shinohara, Appl. Catal. 50 (1989) 119.
[25] A. Benhmid, K.V. Narayana, A. Martin, B. Lücke, Chem. Commun. (2004) 2118.
[26] Patent application submitted to German Patent Office (P241303DE-WT), 2004.
[27] W.-J. Shen, M. Okumura, Y. Matsumura, M. Haruta, Appl. Catal. A 213 (2001) 225.
[28] M. Lyubovsky, M. Pfefferle, A. Datye, J. Bravo, T. Nelson, J. Catal. 187 (1999) 275.
[29] G. Neri, M.G. Musolino, C. Milone, D. Pietropaolo, S. Galvagno, Appl. Catal. A 208 (2001) 307.
[30] D.J. Suh, T.J. Park, S. Ihm, Ind. Eng. Chem. Res. 31 (1992) 1849.
[31] W.S. Epling, G.B. Hoflund, J. Catal. 182 (1999) 5.
[32] A. Benedetti, G. Fagherazzi, F. Pinna, G. Rampazzo, M. Selva, G. Strukul, Catal. Lett. 10 (1991) 215.
[33] C.J. Powell, Appl. Surf. Sci. 89 (1995) 141.
[34] R. Izquierdo, E. Sacher, A. Yelon, Appl. Surf. Sci. 40 (1989) 175.